Proc. Natl. Acad. Sci. USA
Vol. 89, pp. 4139–4143, May 1992
Neurobiology

In vivo imaging of calcium accumulation in fly interneurons as elicited by visual motion stimulation

(optical recording/fura-2/dendritic integration/motion detection)

ALEXANDER BORST AND MARTIN EGELHAAF

Max-Planck-Institut für Biologische Kybernetik, Spemannstrasse 38, W-7400 Tübingen, Federal Republic of Germany

Communicated by Werner Reichardt, January 22, 1992

ABSTRACT **The computation of motion plays a central role in visual orientation. The fly has been successfully used as a model system for analyzing the mechanisms underlying motion detection. Thereby, much attention has been paid to a neuronal circuit of individually identifiable neurons in the third visual ganglion that extracts different types of retinal motion patterns and converts these patterns into specific components of visual orientation behavior. The extended dendritic trees of these large cells are the sites of convergence of numerous spatially distributed local motion-sensitive elements. As is revealed by *in vivo* microfluorometric imaging, these cells accumulate calcium during activation by visual motion stimulation. The spatiotemporal pattern of calcium distribution shows the following characteristics: (*i*) calcium accumulation is first spatially restricted to those dendritic branches that are depolarized by the retinotopic input, (*ii*) during ongoing motion stimulation calcium may also accumulate throughout the cell and, in particular, in regions that do not receive direct synaptic input. These experiments successfully monitor the intracellular distribution of activity-dependent ions in visual interneurons of living animals stimulated by their natural synaptic input.**

Spatial integration of local motion signals is one of the key processing steps in motion vision. Studies of the visual ganglia of insects (1), the middle temporal area of monkeys (2, 3), and the medial superior temporal area (4, 5) of monkeys reveal that spatial integration plays a decisive role in tuning motion-sensitive cells to particular types of retinal motion patterns. This processing step is assumed to be accomplished by the distributed action of large numbers of synapses subserving upstream local motion-sensitive elements. The spatiotemporal characteristics of dendritic integration have so far been analyzed only by conventional electrophysiological techniques. However, optical recording techniques are now available for monitoring the two-dimensional distribution of neuronal activity in single nerve cells. They have been successfully applied to analyze dendritic integration of synaptic input in nerve cells such as hippocampal pyramidal cells or cerebellar Purkinje cells (6–9). For methodological reasons, these studies have been done mostly in cell culture or brain slices rather than in the whole animal (6–9).

As is reported here, optical recording techniques can now also be applied *in vivo* to study dendritic integration of local motion information. Because of their peculiar geometry, the directionally selective motion-sensitive large-field cells in the third visual ganglion of flies (1) are particularly useful for such an analysis. Their dendritic trees are almost two dimensional and are located within a thin superficial layer of the brain. With only minimal dissection of the animal, large parts of their branching pattern can thus be visualized in the focal plane of a microscope after injecting the cells with a fluorescent dye (see Figs. 2*A* and 3*D*). These cells have large receptive fields and receive synaptic input from arrays of retinotopically organized columnar elements. Activation of this input by motion in the preferred direction leads to graded depolarizations of the cell, which may be superimposed by brief spike-like events (see Fig. 1), whereas motion in the opposite or null direction hyperpolarizes the cells (10, 11). The neurons within this network are uniquely identifiable and, therefore, experiments can be done repeatedly on individual neurons in different preparations. Moreover, it is known from extensive electrophysiological and behavioral studies what information of the visual world is coded by these neurons and what functional role they play in visual orientation behavior (1, 12). To study dendritic processing within these neurons by means of optical recording, we have used the fluorescent calcium indicator fura-2 (13), because calcium is probably the most important and ubiquitous messenger linking depolarization of the cell membrane to activation of intracellular biochemical events.

MATERIALS AND METHODS

Animals and Preparation. One- to 2-day-old female blowflies (*Calliphora erythrocephala*) were anesthetized with CO_2 and waxed with their back to a small piece of glass. The legs were cut and the gut was removed. A small window was cut in the back of the head capsule to expose the rear side of the third visual ganglion where the large motion-sensitive neurons reside just below its surface. Further details of the preparation are given elsewhere (14).

Stimuli. The cell was activated by visual motion projected on a translucent hemisphere facing the fly (Fig. 1). The moving patterns were generated mechanically by a rotating striped cylinder with the light source (HBO 100-W mercury arc lamp) placed in its center. The patterns were projected onto the hemisphere from the outside through a series of lenses, apertures, mirrors, and dove prisms. Two pattern windows with diameters of ≈20° could be positioned manually by mirrors on arbitrary sites on the hemisphere in the cell's receptive field. Within the windows the patterns could be moved independently in any direction.

Electrophysiology. Electrodes were pulled on a Brown-Flaming puller (Sutter Instruments, San Francisco) from 1.0-mm tubing (Clarc Electromedical GC100) and were filled with a 12 mM solution of the K^+ salt of fura-2 (Molecular Probes) in 500 mM KCl. They had a resistance of ≈50 MΩ. The indifferent electrode was also used for supply of Ringer's solution (for composition of Ringer's solution see ref. 15). Electrophysiological signals were acquired, stored, and evaluated on an IBM AT computer through an A/D converter (12 Bit, DT2801 A, Data Translation) at 1 kHz. The software was written in ASYST (Keithley) and ensured synchronization with the image acquisition and stimulus control.

Optical Recording. Filled cells were viewed with an upright microscope (Zeiss), a Zeiss UD20 long-distance objective (numerical aperture, 0.56) and an epifluorescence illumina-

The publication costs of this article were defrayed in part by page charge payment. This article must therefore be hereby marked "*advertisement*" in accordance with 18 U.S.C. §1734 solely to indicate this fact.

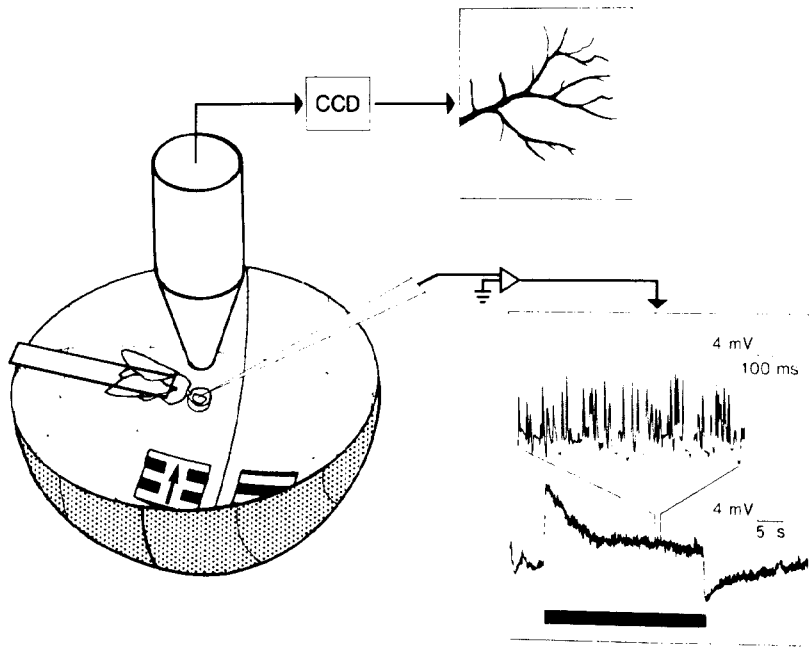

FIG. 1. Experimental setup showing the fly facing a moving stimulus pattern in the inside of a translucent hemispherical screen together with the schematic imaging system. The arrow within the pattern in the ventral part of the fly's visual field indicates that it moves horizontally. A HSE cell is illustrated schematically (*Upper right*) as visualized by the imaging system. (*Lower right*) Electrophysiological responses of this cell. The lower trace represents the membrane potential during motion stimulation in the cell's preferred direction (average from six sweeps). The cell responds mainly with graded membrane potential changes. The response shows a pronounced transient peak at the onset of motion and declines to its steady-state level within 5–10 s. The upper trace is taken from a single sweep of this record and is stretched in time to illustrate the spike-like events superimposed on the graded membrane potential changes. CCD, charge-coupled device.

tion (HBO 100-W mercury arc lamp) with an appropriate filter combination for fura imaging [BP 380 or BP 349 excitation filters (bandwidth, 10 nm), a FT 510 dichroic mirror, and a BP 500–530 barrier filter]. The imaging system (Photometrics, Tucson, AZ) consisted of a Peltier-cooled camera head (CH 250A) with a charge-coupled device chip (PM 512; ultralow dark current; 512 × 512 pixels), an electronic unit (CE 200 A equipped with a 50-kHz 16-bit A/D converter), and a controller board (NU 200). Images were acquired and evaluated by a software package (IPLab, Signal Analytics, Vienna, Va) on a Macintosh IIfx computer (Apple).

Experimental Procedure. The dye was injected into the cell (10–30 min; −1 to −3 nA) until the major cellular processes could be clearly discerned from the background (Fig. 2*A*). After injection of the dye, 10–30 min was allowed for the dye to diffuse throughout the cell before the experiment started. However, the most distal dendritic branches on which most of the input synapses of these cells reside (16) usually could not be recognized in the fluorescence images *in vivo*, as is suggested by a comparison with anatomical data using conventional dyes and sectioned material (15–17). At rest, the fluorescence intensity of the main cell branches was typically 2–5 times higher than background. In some of the experiments, the electrical activity of the cell was simultaneously recorded with an intracellular electrode to ensure that it responded in its normal way (Fig. 1). During the experiments, a sequence of pictures was taken at 1.5-s intervals under epifluorescence illumination of the cell at 380 nm. Five control pictures were taken preceding stimulus presentation followed by 20 images during stimulus motion. Another 15 images were taken after cessation of pattern motion. To determine the resting calcium concentration (13), two pictures were taken with excitation filters centered at 380 (bandwidth, 10 nm) and 349 (bandwidth, 10 nm), respectively, before and after the experiment.

Image Processing. From the raw fluorescence images, the changes in the relative fluorescence ($\Delta F/F$) were determined in the following way. The first picture of the sequence was used as a reference. This picture was subtracted from each picture of the sequence. The resulting difference picture was then divided by the reference picture pixel by pixel. A decrease in $\Delta F/F$ corresponds to an increase in cytosolic calcium concentration (13). Because of movements of the brain that may occur in a living animal, the reference image and successive images may be misaligned, leading to artefacts in the relative fluorescence image. Care was taken to evaluate only those image sequences where these artefacts did not occur or, at least, where they were considerably smaller than the stimulus-induced calcium signals. Compare, e.g., in Fig. 2 *B–D* positive (dark) values to the right of the axon with the signals in the dendrite. The calculation of the change in relative fluorescence described so far does not take into account the contribution of the background to the intensity measured at each image pixel. Therefore, the background must be subtracted to determine the true relative fluorescence change. However, calculation of the $\Delta F/F$ value requires, in this case, a clear distinction of the cellular processes from the background. Otherwise, the denominator may become very small and, hence, the corresponding $\Delta F/F$ value will be extremely prone to noise. We therefore determined the background-corrected $\Delta F/F$ value only for the axon and the main dendritic branches of the cells. For similar reasons, determination of the resting calcium level also requires background subtraction and was consequently calculated only in those regions where the cell could be clearly discerned from background in the raw fluorescence intensity image. Here, the resting calcium concentration was in the range between 20 and 60 nM. From known resting calcium concentration and the background-corrected change in relative fluorescence, the absolute calcium concentration can be calculated for each image frame (ref. 18; V. Lev-Ram, H. Miyakawa, N. Lasser-Ross, and W. N. Ross, personal communication). Variations of the background fluorescence within an image has to be considered as the major source of uncertainty for the values given below. These variations can affect the measurement of the resting calcium concentration

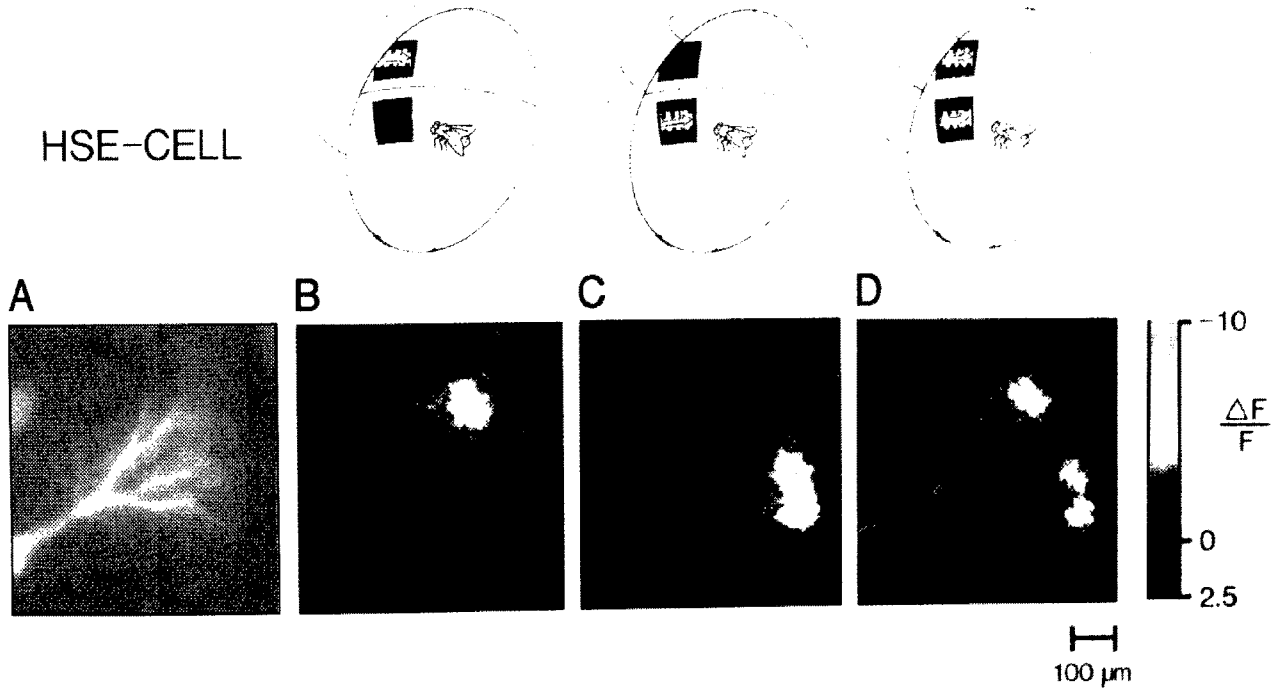

FIG. 2. Preferred direction motion (horizontal motion from the front to the back of the fly) in locally restricted areas (diameter 20°) in the visual field of the fly leads to a locally restricted increase in free cytosolic Ca^{2+} in the dendrites of a motion-sensitive cell (HSE cell). The two stimulus patterns were placed in the receptive field in such a way that they induced membrane potential changes of about the same amplitude when presented alone. (*A*) Fluorescence intensity image (90 × 90 pixels; exposure time, 100 ms) of a HSE cell filled with fura-2 taken at 380 nm excitation in the living animal. (*B–D*) Color-coded changes in the raw relative fluorescence ($\Delta F/F$, without background subtraction) of the same cell at 380 nm excitation (90 × 90 pixels; exposure time, 100 ms) after 9 s of preferred direction motion in the dorsal (*B*), ventral (*C*), and both dorsal and ventral (*D*) parts of the receptive field of the cell. Negative $\Delta F/F$ values correspond to an accumulation of calcium. The stimulus conditions are shown schematically above each image. (Bar = 100 μm.)

as well as the calculation of the change in relative fluorescence, but they are unavoidable because of the inhomogeneous background fluorescence of the *in vivo* preparation.

RESULTS

Motion stimulation leads to localized fluorescence changes in the dendrite. As shown in Fig. 2 *B–D*, an HSE cell (11, 15) was stimulated by horizontal motion of a grating pattern in either the dorsal or the ventral part of its receptive field, respectively, or in both regions simultaneously. The resulting changes in relative fluorescence are shown in Fig. 2 *B–D* after 9 s of motion. The fluorescence changes are restricted to those parts of the dendrite that are activated directly by the retinotopic motion input. During motion stimulation in the dorsal part of the receptive field, there is a calcium response only in the vicinity of one of the main dorsal dendritic branches (Fig. 2*B*). In contrast, when there is motion in the lower part of the cell's receptive field, only areas at the terminals of two ventral dendritic branches indicate an increase in cytosolic calcium. When both patterns move simultaneously, both parts of the dendrite reveal pronounced fluorescence changes (Fig. 2*D*). This experiment has been done in a total of 15 neurons of various types (HS, VS, and CH cells; for the anatomy and functional properties of these cells, see ref. 19). In all cases, a calcium increase was localized in those dendritic regions that correspond to the part of the stimulated visual field. A quantitative estimate of the Ca^{2+} concentration cannot be given here, because this requires the background fluorescence to be subtracted from the image before the relative fluorescence changes are determined (13) (see *Materials and Methods*). Without background subtraction, the relative fluorescence changes might be significantly underestimated. However, those parts of the cell that show the most pronounced fluorescence changes are not the main dendrites but rather the fine distal dendritic branches that cannot be discriminated from the background in the raw fluorescence intensity image (compare Fig. 2*A* with Fig. 2 *B–D*). Nevertheless, the data shown in Fig. 2 *B–D* can at least be compared qualitatively with each other since, within the labeled regions, neither the density of dendritic branching nor the fluorescence intensity of the background varies systematically. Despite the limitations of an *in vivo* preparation, the localized changes in relative fluorescence indicate a local retinotopic calcium accumulation. Hence, this experiment visualizes directly the retinotopic input organization of visual interneurons.

Calcium accumulation may not always remain restricted to the fine branches of the neurons throughout the time of stimulation. In the example shown in Fig. 3, another motion-sensitive cell of the third visual ganglion, a VS1 cell (17, 20), was injected with fura-2 and subsequently stimulated in the ventral part of its receptive field with downward motion (Fig. 3*A*). Fig. 3 *B* and *C* shows the relative fluorescence changes at two instants of time, 6 and 27 s after the stimulus pattern started moving. First, only the ventral branches of the cell's dendrite are labeled (Fig. 3*B*), consistent with the known map of the receptive field on this region. In addition, the major ventral dendrite along with the soma and the axon show some slight labeling. After 27 s (Fig. 3*C*), the labeling has generally increased. Furthermore, it is no longer localized but has spread, in particular to those parts of the dendrite that do not receive synaptic input themselves from the motion stimulus used here. In the experiment shown in Fig. 3 branches of the cell are labeled that can be clearly distinguished from the background in the raw fluorescence images (Fig. 3*E*), and it is possible, therefore, to calculate the background-corrected fluorescence changes in these areas. This was done at five different locations, indicated by windows in Fig. 3*D*. Fig. 3*E* shows the time course of the relative fluorescence change at

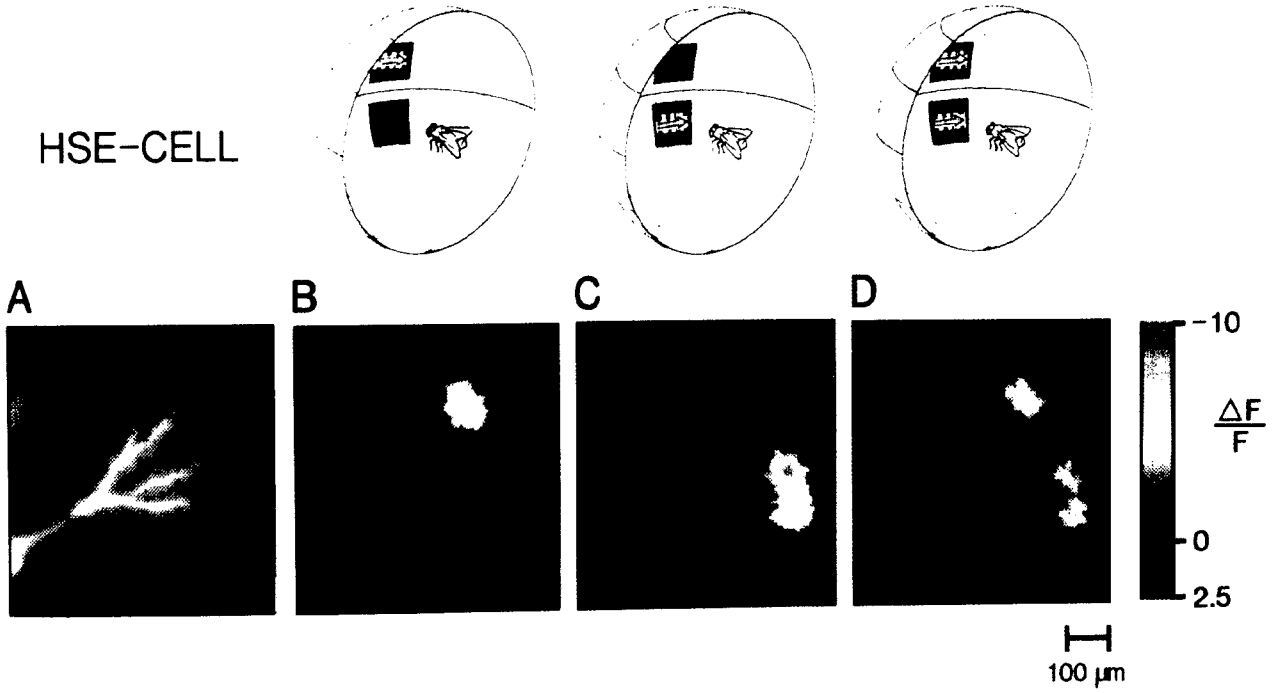

FIG. 2. Preferred direction motion (horizontal motion from the front to the back of the fly) in locally restricted areas (diameter, ≈20°) in the visual field of the fly leads to a locally restricted increase in free cytosolic Ca^{2+} in the dendrites of a motion-sensitive cell (HSE cell). The two stimulus patterns were placed in the receptive field in such a way that they induced membrane potential changes of about the same amplitude when presented alone. (*A*) Fluorescence intensity image (90 × 90 pixels; exposure time, 100 ms) of a HSE cell filled with fura-2 taken at 380 nm excitation in the living animal. (*B–D*) Color-coded changes in the raw relative fluorescence ($\Delta F/F$, without background subtraction) of the same cell at 380 nm excitation (90 × 90 pixels; exposure time, 100 ms) after 9 s of preferred direction motion in the dorsal (*B*), ventral (*C*), and both dorsal and ventral (*D*) parts of the receptive field of the cell. Negative $\Delta F/F$ values correspond to an accumulation of calcium. The stimulus conditions are shown schematically above each image. (Bar = 100 μm.)

as well as the calculation of the change in relative fluorescence, but they are unavoidable because of the inhomogeneous background fluorescence of the *in vivo* preparation.

RESULTS

Motion stimulation leads to localized fluorescence changes in the dendrite. As shown in Fig. 2 *B–D*, an HSE cell (11, 15) was stimulated by horizontal motion of a grating pattern in either the dorsal or the ventral part of its receptive field, respectively, or in both regions simultaneously. The resulting changes in relative fluorescence are shown in Fig. 2 *B–D* after 9 s of motion. The fluorescence changes are restricted to those parts of the dendrite that are activated directly by the retinotopic motion input. During motion stimulation in the dorsal part of the receptive field, there is a calcium response only in the vicinity of one of the main dorsal dendritic branches (Fig. 2*B*). In contrast, when there is motion in the lower part of the cell's receptive field, only areas at the terminals of two ventral dendritic branches indicate an increase in cytosolic calcium. When both patterns move simultaneously, both parts of the dendrite reveal pronounced fluorescence changes (Fig. 2*D*). This experiment has been done in a total of 15 neurons of various types (HS, VS, and CH cells; for the anatomy and functional properties of these cells, see ref. 19). In all cases, a calcium increase was localized in those dendritic regions that correspond to the part of the stimulated visual field. A quantitative estimate of the Ca^{2+} concentration cannot be given here, because this requires the background fluorescence to be subtracted from the image before the relative fluorescence changes are determined (13) (see *Materials and Methods*). Without background subtraction, the relative fluorescence changes might be significantly underestimated. However, those parts of the cell that show the most pronounced fluorescence changes are not the main dendrites but rather the fine distal dendritic branches that cannot be discriminated from the background in the raw fluorescence intensity image (compare Fig. 2*A* with Fig. 2 *B–D*). Nevertheless, the data shown in Fig. 2 *B–D* can at least be compared qualitatively with each other since, within the labeled regions, neither the density of dendritic branching nor the fluorescence intensity of the background varies systematically. Despite the limitations of an *in vivo* preparation, the localized changes in relative fluorescence indicate a local retinotopic calcium accumulation. Hence, this experiment visualizes directly the retinotopic input organization of visual interneurons.

Calcium accumulation may not always remain restricted to the fine branches of the neurons throughout the time of stimulation. In the example shown in Fig. 3, another motion-sensitive cell of the third visual ganglion, a VS1 cell (17, 20), was injected with fura-2 and subsequently stimulated in the ventral part of its receptive field with downward motion (Fig. 3*A*). Fig. 3 *B* and *C* shows the relative fluorescence changes at two instants of time, 6 and 27 s after the stimulus pattern started moving. First, only the ventral branches of the cell's dendrite are labeled (Fig. 3*B*), consistent with the known map of the receptive field on this region. In addition, the major ventral dendrite along with the soma and the axon show some slight labeling. After 27 s (Fig. 3*C*), the labeling has generally increased. Furthermore, it is no longer localized but has spread, in particular to those parts of the dendrite that do not receive synaptic input themselves from the motion stimulus used here. In the experiment shown in Fig. 3 branches of the cell are labeled that can be clearly distinguished from the background in the raw fluorescence images (Fig. 3*E*), and it is possible, therefore, to calculate the background-corrected fluorescence changes in these areas. This was done at five different locations, indicated by windows in Fig. 3*D*. Fig. 3*E* shows the time course of the relative fluorescence change at

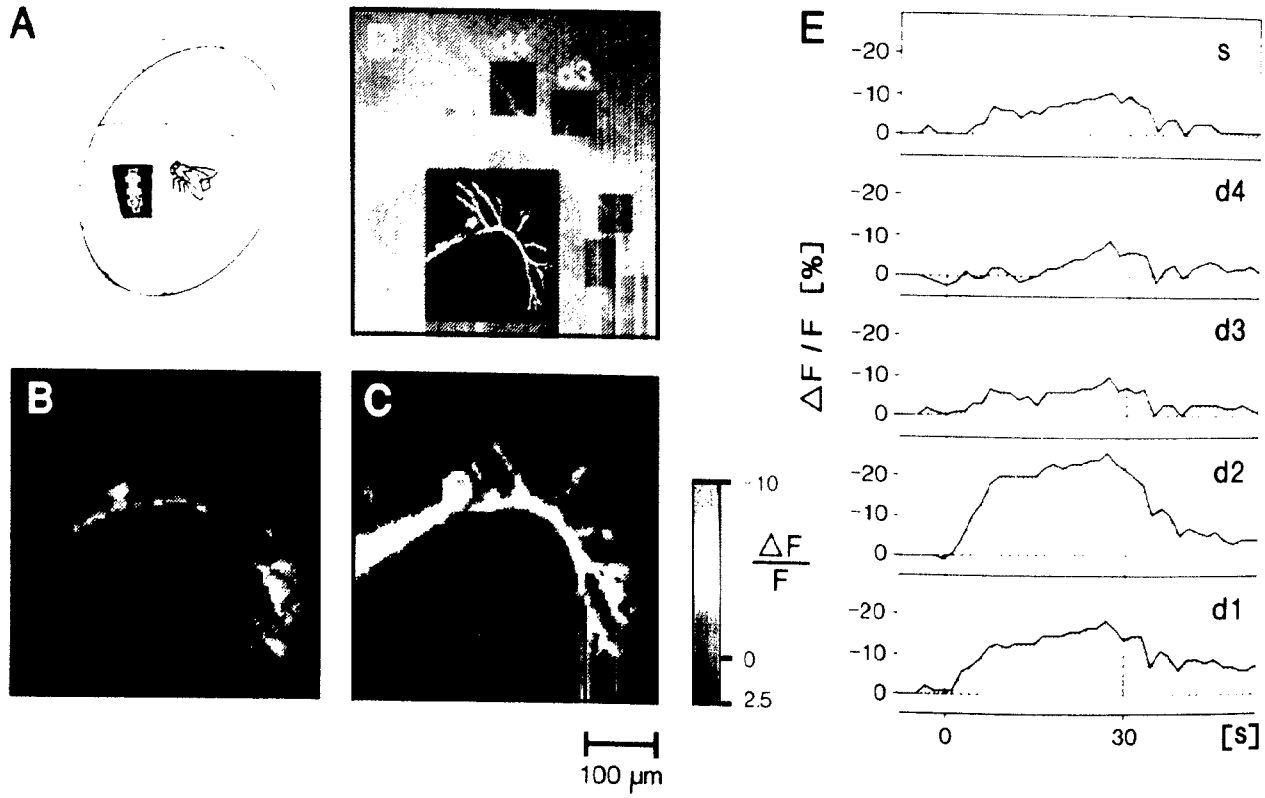

FIG. 3. Long-lasting preferred direction motion stimulation in a locally restricted area of the visual field of the fly leads to an increase in free cytosolic Ca^{2+} throughout the cell (VS1 cell). (*A*) Stimulus condition indicating downward motion in the ventral part of the receptive field of the VS1 cell. (*B* and *C*) Color-coded changes in the raw relative fluorescence ($\Delta F/F$, without background subtraction) of the VS1 cell at 380 nm excitation (100 × 100 pixels; exposure time, 100 ms) after 9 s (*B*) and after 27 s (*C*) of preferred direction motion. (*D*) Fluorescence image of the same cell at 380 nm excitation (100 × 100 pixels; exposure time, 100 ms) together with the windows in which the background-corrected relative change in fluorescence was calculated. (*Inset*) Mask created from the fluorescence image by thresholding the intensity values. (*E*) Time course of the relative change in fluorescence after background subtraction. Within each window indicated in *D*, only those pixels were evaluated that were within the confines of the mask. The pixel values were averaged across each window. Shaded area indicates the time during which the pattern was moving in the cell's preferred direction. The rest of the time the pattern was stationary.

four locations on the dendrite (d1–d4) and the soma (s) of the cell. Calcium accumulation starts in those dendritic branches that are activated during motion stimulation by retinotopic synaptic input (d1 and d2). At these locations, the relative calcium changes are greatest throughout stimulation (≈25%). The change in relative fluorescence of the soma also starts right at the beginning of stimulation. In contrast, the fluorescence signal in the dorsal branches of the cell's dendrite follows with a delay of 10–15 s. The fluorescence signals reach a plateau that is maintained for the duration of the stimulus and subsequently decline to the background level within the next 10–20 s. When the resting Ca^{2+} concentration is known, the background corrected change in relative fluorescence can be transformed into absolute Ca^{2+} concentration (ref. 18; V. Lev-Ram, H. Miyakawa, N. Lasser-Ross, and W. N. Ross, personal communication). This has been done for the data shown in Fig. 3. With respect to a resting Ca^{2+} concentration of 50 mM, a 10% decrease in background-corrected $\Delta F/F$ corresponds to a Ca^{2+} concentration of 84 nM and a 30% decrease in $\Delta F/F$ corresponds to a Ca^{2+} concentration of 185 nM.

DISCUSSION

The data illustrate that the processing of motion information in the dendritic tree of the large-field cells in the third visual ganglion of the fly is accompanied by intracellular calcium accumulation. Calcium rapidly accumulates in those regions of the dendrite that receive direct retinotopic synaptic input (Fig. 2). Preliminary experiments suggest that local Ca^{2+} accumulation depends on the stimulus strength in a graded way. During ongoing stimulation, calcium may also accumulate throughout the cell. In several experiments, the global calcium signal was larger than the initial local transients and developed faster than in the example shown in Fig. 3. Although this has not yet been analyzed quantitatively, it seems that this global signal is triggered by stronger stimulation.

In contrast to the vast amount of data available on the properties of the large-field cells of the fly in response to visual stimulation and on their significance in visual orientation behavior (1, 12), almost nothing is known so far about the ionic basis and the pharmacological characteristics of the ion channels underlying their potential changes. The same is true for the functional role of calcium in the motion-sensitive large-field cells. However, there are two electrophysiological phenomena of these cells that might be linked to calcium regulation. (*i*) Calcium may underlie membrane potential changes such as the spike-like depolarizations (Fig. 1). It is still not clear where in the cell these spikelets are generated. Active membranes in dendrites and, in particular, dendritic spikes have been found recently to be quite common in nerve cells (for review, see refs. 21 and 22). (*ii*) Adaptational changes have been proposed in the motion-detection system of the fly (23–25). Calcium may act as a second messenger that controls these changes in the sensitivity of the cell to motion stimulation, for instance, by activating calcium-dependent potassium channels. By comparing the dynamic properties of the large-field cells and their local motion-detecting input elements (14, 26), at least part of the decline in response amplitude in the large-field cells during maintained motion stimulation (Fig. 1) may be due to such

adaptational changes. Interestingly, these changes have a time course that is reminiscent of the time course of calcium accumulation in the cell (compare Fig. 1 *Lower right* and Fig. 3*F*). Future experiments with photolabile calcium cages (27, 28) should reveal whether calcium does indeed modulate the sensitivity of the cell to motion stimulation.

We are grateful to M. Dickinson, K. G. Götz, W. Reichardt, and two anonymous referees for useful comments on the manuscript; to W. Ross and D. Tank for technical advice concerning the use of fura-2; and to S. Flecks and A. Wildemann for excellent technical assistance.

1. Hausen, K. & Egelhaaf, M. (1989) in *Facets of Vision*, eds. Stavenga, D. G. & Hardie, R. C. (Springer, Berlin), pp. 391–424.
2. Mikami, A., Newsome, W. T. & Wurtz, R. H. (1986) *J. Neurophysiol.* **55,** 1308–1327.
3. Rodman, H. R., Gross, C. G. & Albright, T. D. (1989) *J. Neurosci.* **9,** 2033–2050.
4. Tanaka, K., Fukada, Y. & Saito, H. (1989) *J. Neurophysiol.* **62,** 642–656.
5. Tanaka, K. & Saito, H. (1989) *J. Neurophysiol.* **62,** 626–641.
6. Tank, D. W., Sugimori, M., Connor, J. A. & Llinas, R. R. (1988) *Science* **242,** 773–777.
7. Ross, W. N., Lasser-Ross, N. & Werman, R. (1990) *Proc. R. Soc. London B* **240,** 173–185.
8. Regehr, W. G., Connor, J. A. & Tank, D. W. (1989) *Nature (London)* **341,** 533–536.
9. Ross, W. N., Arechiga, H. & Nicholls, J. G. (1987) *J. Neurosci.* **7,** 3877–3887.
10. Hengstenberg, R. (1977) *Nature (London)* **270,** 338–340.
11. Hausen, K. (1982) *Biol. Cybern.* **46,** 67–79.
12. Egelhaaf, M., Hausen, K., Reichardt, W. & Wehrhahn, C. (1988) *Trends Neurosci.* **11,** 351–358.
13. Grynkiewicz, G., Poenie, M. & Tsien, R. Y. (1985) *J. Biol. Chem.* **260,** 3440–3450.
14. Egelhaaf, M., Borst, A. & Reichardt, W. (1989) *J. Opt. Soc. Am. A* **6,** 1070–1087.
15. Hausen, K. (1982) *Biol. Cybern.* **45,** 143–156.
16. Hausen, K., Wolburg-Buchholz, K. & Ribi, W. A. (1980) *Cell Tissue Res.* **208,** 371–387.
17. Hengstenberg, R., Hausen, K. & Hengstenberg, B. (1982) *J. Comp. Physiol. A* **149,** 163–177.
18. Vranesic, I. & Knöpfel, T. (1991) *Pflügers Arch.* **418,** 184–189.
19. Hausen, K. (1984) in *Photoreception and Vision in Invertebrates*, ed. Ali, M. A. (Plenum, New York), pp. 523–559.
20. Hengstenberg, R. (1982) *J. Comp. Physiol. A* **149,** 179–193.
21. Llinas, R. R. (1988) *Science* **242,** 1654–1664.
22. Hounsgaard, J. & Midtgaard, J. (1989) *Trends Neurosci.* **12,** 313–315.
23. Maddess, T. & Laughlin, S. B. (1985) *Proc. R. Soc. London B* **225,** 251–275.
24. de Ruyter van Steveninck, R., Zaagman, W. H. & Mastebroek, H. A. K. (1986) *Biol. Cybern.* **53,** 451–463.
25. Borst, A. & Egelhaaf, M. (1987) *Biol. Cybern.* **56,** 209–215.
26. Egelhaaf, M. & Borst, A. (1989) *J. Opt. Soc. Am. A* **6,** 116–127, and erratum (1989) **7,** 172.
27. Tsien, R. Y. (1988) *Trends Neurosci.* **11,** 419–424.
28. Kaplan, J. H. & Somlyo, A. P. (1989) *Trends Neurosci.* **12,** 54–59.